International Journal of Signal Processing, Image Processing and Pattern Recognition
Vol. 8, No. 1 (2015), pp. 69-78
http://dx.doi.org/10.14257/ijsip.2015.8.1.07

Image Fusion Watermarking Algorithm based on NSCT and Constrained NMF

Xianmin Wei[1] and Peng Zhang[2]

[1,2]*School of Computer Engineering, Weifang University*
5147 Eastern Dongfeng Street, Weifang 261061, China
wfxyweixm@126.com

Abstract

In order to solve the problem aliasing of Contourlet transform, an Image Fusion Watermarking Algorithm based on NSCT and constrained NMF is proposed in this paper. Firstly, the image is decomposed into several layers. Secondly, the Two-dimension matrix is obtained by low frequency coefficients and watermarking signal. Finally, the watermarking is embedding by constrained NMF. The blind detection is used, and the algorithm can achieve a good imperceptibility. Experimental results show that the algorithm has good robustness against attacks of common image processing.

Keywords: *Digital watermarking, Non-subsampled Contourlet Transform (NSCT), Non-negative Matrix Factorization (NMF), Image fusion*

1. Introduction

Features of digital images easily spread and replicated have made worse image content infringing, tampering, forgery and other growing problem, the image content information security has become a problem to be solved lately. Digital watermarking is a technology embedded in the multimedia data having imperceptible, robust, resisting detectability and which contains digital coding technology of sensitive information authentication, mainly used for addressing the identification mark provided in digital media copyright protection problem [1]. As an emerging discipline, the digital watermarking in the communications, computer, cryptography has achieved a wide range of applications, which is an effective way to solve the above problems.

In 2002, M.N.Do and M. Vetteri [2, 3], who proposed the outline wave-Contourlet transform, Contourlet transform is a real image two-dimensional representation, which provides a flexible multi-scale, local, directional the analytical method, and which can more fully demonstrate the geometric characteristics of the image itself. Contourlet transform will be applied once appeared in the field of digital watermarking, and made a series of studies [4, 5]. But smoothness of Contourlet transform basis functions is not ideal; spectrum aliasing exists in low-frequency sub-band, high-frequency sub-band and each directional sub band. In 2006, for some limitations A.L.Cunha improved Contourlet transform, and proposed a non-sampling Contourlet Transform (Non-subsampled Contourlet Transform, NSCT) [6] method, NSCT is a shift-invariant, multi-scale, multi-direction super complete transformation [7], compared with Contourlet transform, smooth and high NSCT basis functions has no spectral aliasing, and it has stronger direction selectivity.

For presence of confusion problem in Contourlet transform spectrum, this paper designed a fusion of non-sampling Contourlet transform watermark and constraints NMF algorithm based on a combination of image. Watermark information by NMF embedded into the image fusion among NSCT decomposition coefficients. Compared with the traditional NMF, constrained NMF has low computational complexity, good separation

ISSN: 2005-4254 IJSIP

and unique decomposition. Simulation results show that the algorithm is more robust and larger embedding capacity.

2. Contourlet and NSCT

Contourlet transform, also known as pyramid directional filter bank (pyramidal directional filter bank, PDFB), is a multi-scale non-separated representation of the signal. PDFB first performed LP (Laplacian pyramid) transformation [8] and multi-scale analysis to capture the singular point in image; then the direction filter bank DFB (directional filter bank) will synthesize one coefficient using singular points distributed in the same direction, this structure makes Contourlet transform nonlinear approximation with optimum performance. PDFB and DFB filtering repeated on a rough image, so the image is decomposed into multi-scale directional sub-band. Figure 1 and Figure 2 show the diagrams and scale orientation distribution of Contourlet transform image decomposition process.

Contourlet transform is a new extension of wavelet transforms, with the nature of multi-resolution, local location, multi-directional, and anisotropic sampling neighbor sector, its basis functions distributed in multi-scale and multi-direction, a small range of coefficient can effectively capture the image edge contour. However, as in the Contourlet transform, Laplace pyramid decomposition in bandwidth-dimensional separable bi-orthogonal filter banks are larger than π / 2, based on multi-rate theory, image has spectrum aliasing after filtered and then after every column interlaced. The following sample generates spectral confusion in Contourlet transform low-frequency sub-bands and high-frequency sub-bands. The direction of each directional sub-band filter bank is the result of the formation of the high frequency sub-band, there is also the spectrum aliasing.

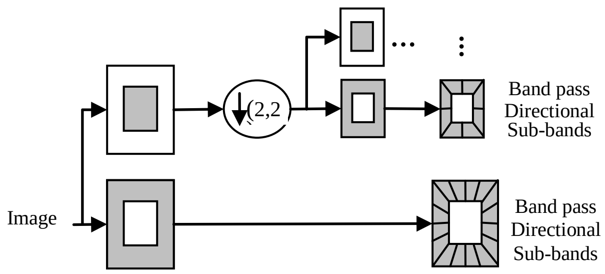

Figure 1. Contourlet Transform Decomposition

In order to eliminate spectral aliasing of Contourlet transform and enhance its direction selectivity, [6] proposed a tower NSCT structure by the decomposition without down-sample(NSP) and non-subsample directional filter bank (NSDFB), its structure shown in Fig.3. NSDFB is an equivalent translocation relation to remove formation after the DFB in the next sampling operation. Since the NSP and NSDFB without down-sample operation, so NSCT with translation invariance. Since there is no link in the tower sampling decomposition process, even if the filter bandwidth is greater than π / 2, its low frequency sub-band spectrum would not be confused with the phenomenon.

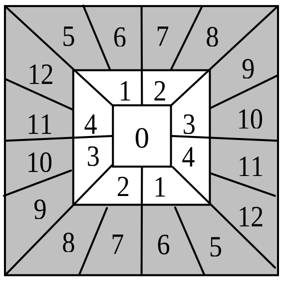

Figure 2. Distributed Diagram of Contourlet Transform Scale and Direction

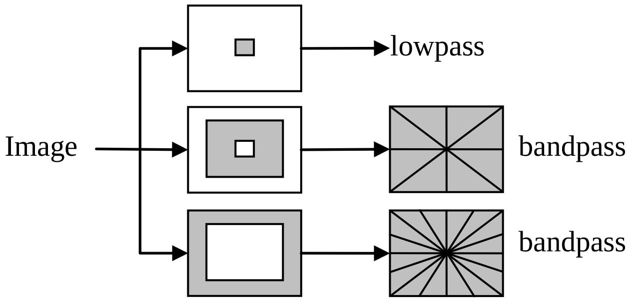

Figure 3. NSCT Structure Diagram

3. NMF

Non-negative Matrix Factorization (NMF) was proposed by Lee and Seung [9] in 1999 in Nature, and proved the convergence of the algorithm in 2000. After all components decomposition with non-negative value, the pure additive claim description, and while the nonlinear dimensionality reduction defined as follows:

Definition: an M-dimensional vector v after N times random observations, $v_j, j = 1,2,\cdots,N$, $V = [V_{\cdot 1}, V_{\cdot 2}, \cdots, V_{\cdot N}]$. Where $V_{\cdot j} = v_j, j = 1,2,\cdots,N$, which requires the existence of non-negative base matrix $M \times L$, $W = [W_{\cdot 1}, W_{\cdot 2}, \cdots, W_{\cdot N}]$ and coefficients matrix $L \times N$, $H = [H_{\cdot 1}, H_{\cdot 2}, \cdots, H_{\cdot N}]$, so $V \approx WH$ [9,10].

Usually $L \leq \min(M, N)$ required, that is when W contains the essential characteristics of random variables, to use fewer base to describe a large number of sample data to make an expression $V \approx WH$. The key is to choose the algorithm and iterative rule setting the objective function, commonly used objective function and iterative rules are as follows:

The objective function: Minimize $\|V - WH\|^2$, for any W and H, when $W, H \geq 0$, the iteration rule:

$$H_{kj} \leftarrow H_{kj} \frac{(W^T V)_{kj}}{(W^T WH)_{kj}}, W_{ik} \leftarrow W_{ik} \frac{(VH^T)_{ik}}{(WHH^T)_{ik}} \quad (1)$$

In order to get good separation performance and the only results of W and H, this paper will be bound by the determinant criterion for H sparse and relevance constraints to balance the reconstruction error, the uniqueness of the mixing matrix W, the coefficient matrix H sparse and correlation, this paper uses the literature [11] iteration rule:

$$H_{kj} = H_{kj}\left(\frac{[W^T V]_{kj} - \alpha_J - \alpha_R\left(\frac{h_{kj}}{(h_k h_k^T)} - [(HH^T)^{-T} H]_{kj}\right)}{[W^T WH]_{kj} + \varepsilon}\right) \quad (2)$$

$$W_{ik} = W_{ik}\left(\frac{[VH^T]_{ik}}{[WHH^T]_{ik} + \varepsilon} - \alpha_W \det(WW^T)\frac{[(WW^T)^{-1} W]}{[H^T HW]_{ik} + \varepsilon}\right) \quad (3)$$

Where ε is a small normal ripening to prevent the denominator is zero. After each iteration step the negative elements of W and H are set to $W_{ik} = \frac{W_{ik}}{\sum_k W_{ik}}$ zero, and is used for the column vectors of W normalization of iterations until less than a preset threshold, the convergence of the algorithm is considered, only W and H obtained at this time.

4. Watermarking Algorithm

4.1. Embedding Watermark

This designed algorithm for the carrier image I, size is $M \times M$. Watermark sequence $WM = \{w_1, w_2, \cdots, w_L\}$ is generated by a user key U and obey the pseudo-random sequence. Embedding flowchart shown in Figure 4. The core watermark embedding algorithm programmed shown as follows:

```
Image = imread ('image.jpg'); % read in the image and preprocessing
im=rgb2gray(im);
im=imresize(im,[256,256]); % NSCT decomposition parameters
nlevels = [0, 1, 3];% decomposition series
pfilter = 'maxflat';% pyramid filter parameters
dfilter = 'dmaxflat7';% directional filter parameters
coeffs = nsctdec (double (image), nlevels, dfilter, pfilter);% NSCT decomposition
lowcoeffs = coeffs {1};% extract low frequency sub-band coefficients
templow = lowcoeffs (:);% low frequency sub-band coefficients of one-dimensional
pn = 123456;% user key rand ('seed,' pn)
WM = rand (256,256); % generate random watermark sequence
P = [templow WM]; % low-pass coefficients with watermark sub-graph integration
[WH] = nmf (P); % NMF decomposition
Save HH; % save sparse matrix H is used to extract the watermark
minw = min (W);
maxw = max (W);
W = ((W-minw) / (maxw-minw)) * 255;
lowcoeffs = reshape (W, [256,256]);
coeffs {1} = lowcoeffs;
imrec = nsctrec (coeffs, dfilter, pfilter);% NSCT reconstruction
```

Specific embedded steps as follows:

(1)Ooriginal image I_0 is in NSCT transform, the low-pass I_J and band-pass sub-picture $d_{j,k}^{l_j}, k = 0,1,\cdots,2^{l_j - 1}, j = 1,2,\cdots,J$, where j represents LP decomposition at the j-th stage, k represents DFB directional sub-band decomposition of l_j at the k-th stage;

(2) Low-pass one-dimensional sub-picture I_J, in combination with the watermark sequence into $L \times 2$ matrix $P = [I_L, W_L]$;

(3) Non-negative matrix P is in NMF constrain decomposition, series coefficient r = 1, the result was $[W, H]$, compressed sparse matrix H is used to save the watermark extraction;

(4) Re-modeling the coefficient matrix W into 2-dimensional matrix and through NSCT reconstruction obtaining NSCT watermarked image I_W, algorithm flow chart shown in Figure 4.

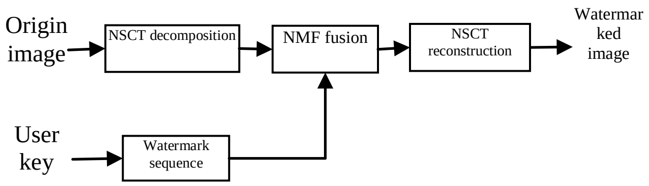

Figure 4. Flow Chart Watermarked Embedding Algorithm

4.2. Watermark Extraction

Watermark extraction process is the reverse process of the watermark embedding process, watermark embedding algorithm core programming as follows:

```
% NSCT decomposition parameters
nlevels = [0, 1, 3];% decomposition series
pfilter = 'maxflat';% pyramid filter parameters
dfilter = 'dmaxflat7';% directional filter parameters
coeffs = nsctdec (double (imrec), nlevels, dfilter, pfilter);% NSCT decomposition
lowcoeffs = coeffs {1};% extract low frequency sub-band coefficients
pn = 123456;% user key rand ('seed,' pn)
WM = rand (256,256); % original watermark sequences generated
rou = (sum (lowcoeffs. * (WM))) / (256 * 256);% rou correlation values for the detection
of the watermark
```

Watermark extraction process is described below in detail:

(1) Watermarked image $I_W^{'}$ under NSCT decomposition, taking the low-pass sub-band coefficients $I_J^{'}$ and one-dimensional;

(2) According to the matrix operation rules, the extracted watermark sequence of W ';

(3) Hypothesis testing based on maximum likelihood estimation watermark correlation detection, correlation value is $\rho = \frac{1}{MN}\sum_{i=1}^{M}\sum_{j=1}^{N}\tilde{C}(i,j)W(i,j)$, according to the Neyman-Pearson criterion $P_f \le \frac{1}{2} erfc\left(\frac{T_p}{\sqrt{2\sigma_\rho^2}}\right)$; Assuming $P_f = 10^{-6}$, $T_\rho = 3.36\sqrt{2\sigma_\rho^2}$, $\sigma_\rho^2 = \frac{1}{MN}\cdot\sum_{i=1}^{M}\sum_{j=1}^{N}(\tilde{C}(i,j))^2$.

5. Simulation Test

5.1. Robustness Analysis

MATLAB7.0 was used in algorithm simulation software platform, the carrier image was selected gray scale image 256×256, the user key generated a random watermark sequences. Original image and watermarked images are shown in Figure 5 (a) and (b) below. Using Stirmark4.0, Photoshop CS and other tools to achieve the watermarked image common attacks, containing the portion result of the attack of the watermarked image shown in Figure 6. The watermark extraction results under a variety of attacks shown in Tables 1 and 2. Superior performance under attack from Table 1 compared with the algorithm

LATESTRNDDIST_1.1, AFFINE_2, NOISE_20, Sharp and [12], the performance in the rest of the attack is also more stable, while [12] is not given in JPEG40, experimental results PSNR_50, SS_2 under attacks. From Table 2, except in the strength of the algorithm under attack twisted corrugated performance slightly below 500[13], the performance of the rest of the attack is higher than [12, 13], results show that this algorithm has a strong anti-local nonlinear geometric attacks [14, 15].

$$NC = \frac{\sum_{i=1}^{L} w(i)^{'} w(i)}{\sqrt{\sum_{i=1}^{L} w(i) \times w(i)} \sqrt{\sum_{i=1}^{L} w^{'}(i) \times w^{'}(i)}} \tag{4}$$

Where, $w(i)$ and $w^{'}(i)$ represent origin watermarking sequence and extracted watermark sequence respectively.

(a)Carrier Image (b)Watermarked Image

Figure 5. Origin Image and Watermarked Image

(*a*)NOISE_20 (*b*)LATESTRNDDIST_1.1 (*c*)AFFINE_2 (*d*)RML_70

(*e*)Corrugated distortion (*f*)Extruding distortion (*g*)Spherical distortion (*h*)Ripple distortion

(*h*)MEDIAN_5 (*i*)RNDDIST_1.1 (*j*) Triangular wave (*k*) Sine wave

Figure 6. Partly Tested Images

Table 1. Anti-Stirmark Attack Data

	PSNR(dB)	Ref. [12]*NC*	*This NC*
LATESTRNDDIST_1.1	15.2	0.6667	0.7999
AFFINE_2	13.09	0.7941	0.7946
RESC_110	25.69	0.9118	0.7863
RML_70	25.61	0.9118	0.7783
MEDIAN_5	25.78	0.8235	0.7823
NOISE_20	4.78	0.4412	0.7875
RNDDIST_1.1	14.66	0.8529	0.8055
ROT_0.75	15.56	0.8235	0.7985
ROTCROP_2	13.55	0.8529	0.7802
ROTSCALE_0.25	25.83	0.8529	0.7838
JPEG40	31.52	--	0.7858
PSNR_50	25.86	--	0.7852
SS_2	1.39	--	0.8594
Sharp	21.69	0.8235	0.8840

Table 2. Anti-local Nonlinear Geometric Attacks

	PSNR(dB)	Ref.[12]*NC*	Ref.[13]*NC*	*This NC*
Corrugated distortion 500	18.79	0.7931	0.92	0.8837
Extruding distortion 50	16.23	0.6190	0.67	0.8952
Spherical distortion 50	14.74	0.6552	0.51	0.8769
Ripple distortion 10	19.41	0.8276	0.73	0.9101
Rotate distortion 50	16.35	0.4688	0.53	0.8957
Sine wave	15.46	0.5313	0.7658	0.9008
Triangular wave	19.18	0.6364	0.968	0.8720
Square wave	14.26	0.6786	0.73	0.9363

5.2. Security Analysis

This designed security of the algorithm depends on the user key U; different users will use key U_i to generate a different watermark sequences, the subscript I represents different users. To verify the security of the algorithm, the 1000 user keys were randomly generated by generation 1000 groups of watermark sequences. Similarity between the random user keys U_i and the original extraction watermark shown in Figure 7. In Figure 7, the horizontal axis is randomly generated 1000 groups of independent pseudo-random binary sequence, the vertical axis is the NC value, to facilitate the comparison group setting 500th original user key. Respectively, using the pseudo-random sequence and a user key k watermark extraction, the decision threshold T = 0.76, the proposed method can be seen to be sensitive to the user key.

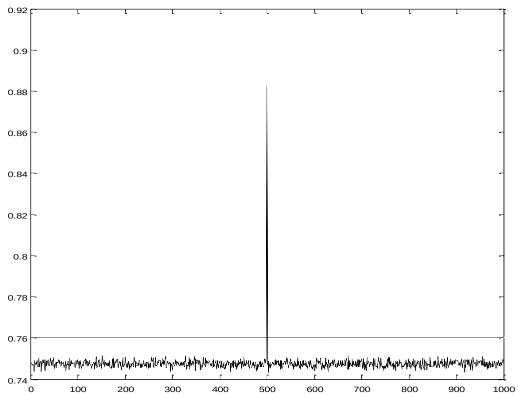

Figure 7. Algorithm Security Analysis

6. Conclusions

This paper attempts to combine non-sample Contourlet transform with constraint NMF into the field of digital watermarking, using low-frequency sub-band coefficients NMF in image NSCT decomposition to achieve integration embedded watermark information. NMF constraint reduces the amount of computation, decomposition is unique. Experimental results show that the algorithm is invisible watermark in ensuring the premise, with a larger embedding capacity and robustness. In future work, to further improve the NMF constraints, making the watermarking algorithm better balance between invisibility and robustness. Also further analysis is needed for algorithm in a larger-scale attack strength and robustness.

Acknowledgements

This work is partly supported by National Natural Science Foundation of China (No. 61471269), Shandong Spark Program (2012XH06005), Weifang municipal Science and Technology Development Program (201301050) and the doctoral scientific research foundation of Weifang University (2104BS12).

References

[1] W. Yan, W. Jianjun and H. Xuming, "Polygon curve watermarking algorithm based on ICA", Computer-Aided Design and Computer Graphics, vol. 18, no. 7, **(2006)**.
[2] M. N. Do and M. Vetterli, "The contourlet transform: an efficient directional multiresolution image representation", IEEE Transactions on Image Processing, vol. 14, no. 6, **(2005)**.
[3] D. Po Duncan and M. N. Do, "Directional multiscale modeling of images using the contourlet transforms", IEEE Transactions on Image Processing, vol. 15, no. 6, **(2006)**.
[4] L. Haifeng, S. Weiwei and W. Shu-xun, "Robustness of image watermarking algorithm based on Contourlet transform", Communications, vol. 27, no. 4, **(2006)**.
[5] B. Nadia, "Adaptive watermarking schemes based on a redundant contourlet transform", Proceedings of the International Conference on Image Processing, Genoa, vol. 1, **(2005)**, pp. 221-224.
[6] A. L. Cunha, J. P. Zhou and M. N. Do, "The no subsampled Contourlet transform: theory, design and applications", IEEE Trans on Image Processing, vol. 15, no. 10, **(2006)**.
[7] Q. Xiaobo, Y. Jing Wen and Y. Guide, "Laplace improve energy and sharp frequency localized Contourlet domain image fusion method", Optics and Precision Engineering, vol. 17, no. 5, **(2009)**.
[8] N. D. Minh and V. Martin, "Framing Pyramids", IEEE Transactions Signal Processing, vol. 51, no. 9, **(2003)**.
[9] D. D. Lee and H. S. Seung, "Learning the parts of objects by non-negative matrix factorization", Nature, vol. 401, **(1999)**.
[10] L. Le and Y.-Jin, "Summary NMF algorithm", Journal of Electronics, vol. 36, no. 4, **(2008)**.
[11] Z. Zhi-Jin, L. Wang and S. Junnuo, "Constraint-based NMF underdetermined blind signal separation algorithm", Computer Applications Research, vol. 28, no. 5, **(2011)**.

[12] C. De Long, Z. King Long and P. Zhiping, “Focus on local nonlinear geometric attacks anti-watermarking algorithm”, Computer Applications, vol. 30, no. 8, **(2010)**.
[13] L. Jingbing, “Watermarking algorithm transform domain-based anti-geometric attacks”, Chongqing University PhD thesis, **(2007)**.
[14] Y. E. Jun and J. Zhong, “Smoothed l_0 norm constrained nonnegative matrix factorization on orthogonal subspace”, Application Research of Computers, vol. 3, no. 35, **(2013)**.
[15] Q. Hanli and M. Changfeng, “An energy extraction method to determine the base number in NMF”, Journal of Guilin University of Electronic Technology, vol. 6, no. 15, **(2012)**.

Authors

Xianmin Wei, he received the M. Sc. degree in computer applications from Shandong Science and Technology University (2005). He is currently an associate professor in school of computer engineering at Weifang University, China. He has published over 30 papers and 3 books in professional fields. Since 2011, he has been a member of IEEE-CS, ACM and CCCF, respectively. His fields of research are focused on swarm intelligent, intelligent sensor networks.

Peng Zhang, he received his PhD degree of communication and information systems from Shandong University, Jinan, P. R. China, in December 2012. Currently, he is a lecturer in the School of Computer Engineering, Weifang University, Shandong, P. R. China. His current research interests focus on advanced coded modulation, massive MIMO, spatial modulation, cross-layer design, cooperative communications and 4G/B4G wireless communications.